Examining a reduced jet-medium coupling in Pb+Pb collisions at the Large Hadron Collider

Barbara Betz and Miklos Gyulassy

Phys. Rev. C **86**, 024903 — Published 6 August 2012

DOI: 10.1103/PhysRevC.86.024903

The reduced jet-medium coupling in Pb+Pb collisions at the Large Hadron Collider

Barbara Betz[a] and Miklos Gyulassy[b]
[a] *Institute for Theoretical Physics, Johann Wolfgang Goethe-University, 60438 Frankfurt am Main, Germany*
[b] *Department of Physics, Columbia University, New York, 10027, USA*

Recent data on the nuclear modification factor R_{AA} of jet fragments in 2.76 ATeV Pb+Pb collisions at the Large Hadron Collider (LHC) indicate that the jet-medium coupling in a Quark-Gluon Plasma (QGP) is reduced at LHC energies and not compatible with the coupling deduced from data at the Relativistic Hadron Collider (RHIC). We estimate the reduction factor from a combined fit to the available data on $R_{AA}(\sqrt{s}, p_T, b)$ and the elliptic flow $v_2(\sqrt{s}, p_T, b)$ at $\sqrt{s} = 0.2, 2.76$ ATeV over a transverse momentum range $p_T \sim 10 - 100$ GeV and a broad impact parameter, b, range. We use a simple analytic "polytrop" model ($dE/dx = -\kappa E^a x^z T^c$) to investigate the dynamical jet-energy loss model dependence. Varying $a = 0 - 1$ interpolates between weakly-coupled and strongly-coupled models of jet-energy dependence while $z = 0 - 2$ covers a wide range of possible jet-path dependencies from elastic and radiative to holographic string mechanisms. Our fit to LHC data indicates an approximate 60% reduction of the coupling κ from RHIC to LHC and excludes energy-loss models characterized by a jet-energy exponent with $a > 1/3$. In particular, the rapid rise of R_{AA} with $p_T \geq 10$ GeV combined with the slow variation of the asymptotic $v_2(p_T)$ at the LHC rules out popular exponential geometric optics models ($a = 1$). The LHC data are compatible with $0 \leq a \leq 1/3$ pQCD-like energy-loss models where the jet-medium coupling is reduced by approximately 10% between RHIC and LHC.

I. INTRODUCTION

First data from the Large Hadron Collider (LHC) on the nuclear-size dependence of jet-medium interactions in Pb+Pb collisions at $\sqrt{s} = 2.76$ ATeV [1–14] showed that the jet-medium coupling at the LHC is weaker than expected [15–18] from fixed coupling extrapolations from $\sqrt{s} = 0.2$ ATeV data at the Relativistic Heavy Ion Collider (RHIC) [19–23]. From the factor of ~ 2 increase of global multiplicity per unit rapidity, $dN_{\rm ch}/d\eta \approx 1600$ in central Pb+Pb reactions at the LHC relative to RHIC, substantially more suppression of high-p_T pions was predicted than observed. In this paper we estimate the reduction of the the jet-medium coupling implied by the new data and test the consistency for a wide variety of jet-energy loss models.

An open question from studies of the nuclear modification factor of jets at RHIC is whether jet-medium interactions in dense deconfined Quark-Gluon Plasma (QGP)-matter can be better described in terms of weakly-coupled perturbative QCD (pQCD) tomography or novel strongly-coupled gravity-dual Anti-de-Sitter/Conformal Field Theory (AdS/CFT) string-model holography [24–26]. The first data from LHC provide stringent new tests of jet-medium interaction models for a higher QGP-density range and for an order of magnitude higher transverse momentum range. The doubling of the QGP density at LHC relative to RHIC extends the temperature range by approximately 30% beyond the range explored at RHIC.

In order to extract either tomographic or holographic information from the jet-quenching observable systematics, it is important to specify the initial jet flux at the jet-production points and the initial geometry of the QGP medium. Two competing models, the Glauber [27] model and the Color Glass Condensate (CGC) [28], have been used so far describe the initial QGP medium geometry and to predict the impact parameter b and beam energy $\sqrt{s}$ dependence of those distributions. The Glauber model is based on an eikonal Wood-Saxon nuclear geometry and assumes incoherent superposition of proton-proton collisions while CGC models are based on non-linear, small-x saturation effects [29–31]. Here, we calculate jet-quenching observables using both initial geometries as a measure of current systematic theoretical errors associated with uncertainties of the initial QGP geometries as a function of impact parameter.

In this paper, we use a simplified analytic "polytrop" jet-energy-loss model [32, 33] that can interpolate between a wide class of weakly and strongly-coupled models of jet-medium interaction in high-energy nuclear collisions:

$$\frac{dP}{d\tau}(\vec{x}_0, \phi, \tau) = -\kappa P^a(\tau)\, \tau^z\, T^c[\vec{x}_\perp(\tau), \tau; b]\ . \qquad (1)$$

The energy loss per unit length is characterized by the three exponents (a, z, c) that determine the jet-energy dependence P^a, the path-length dependence τ^z, and the local temperature-power dependence $T^c(\vec{x}_\perp, \tau)$. This polytrop model reproduces the results of detailed Djordjevic-Gyulassy-Levai-Vitev (DGLV) opacity series calculations remarkably well [15, 17] but has the advantage of allowing quick estimates of the variations of predictions to even large deformations of dynamical assumptions.

The energy loss per unit length, $dE/dx = dP/d\tau$ depends on the local proper time τ in a frame where the jet rapidity y vanishes. The jet path is thus perpendicular to the beam axis in that frame and can be assumed to be straight eikonal line $\vec{x}_\perp(\tau) = \vec{x}_0 + \hat{n}(\phi)\tau$ from the production point $\vec{x}_0$ in direction of the jet azimuthal angle ϕ relative to the reaction plane $\hat{b}$. Bjorken longitudinal expansion [38] is taken into account by $T(\vec{x}, \tau) =$

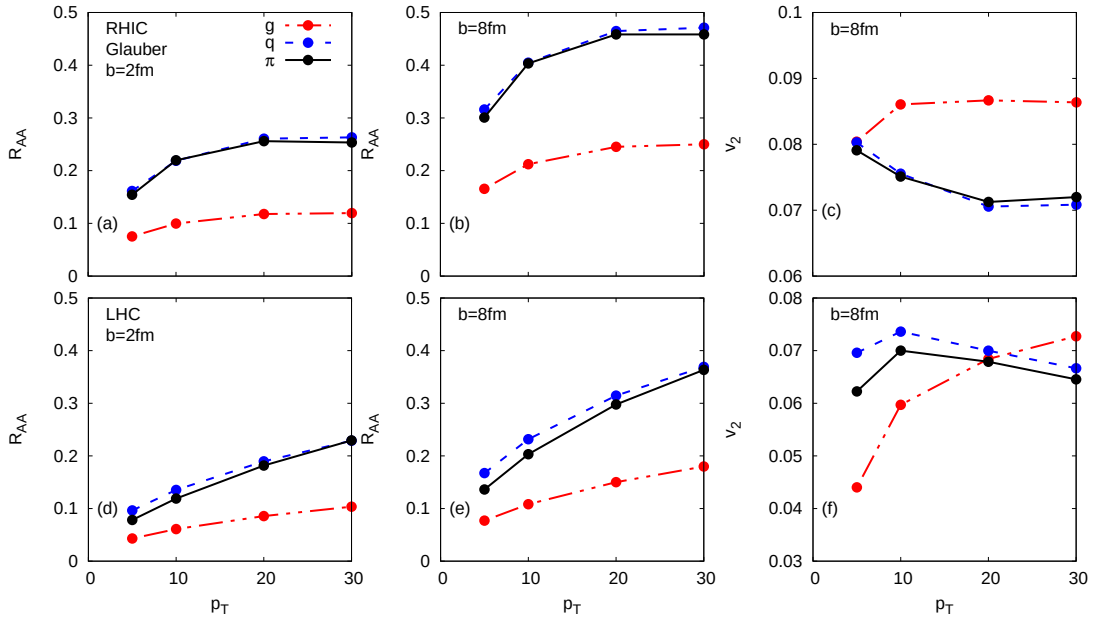

FIG. 1: (Color online) Illustration of the remarkable similarity of quenched pion R_{AA} and v_2 (solid black line) to the underlying quark-jet nuclear modification (blue dashed lines) and the approximate independence of pion nuclear modification factor on the much higher quenched gluon jets (red dashed-dotted lines) at both RHIC (upper panels) and LHC (lower panels). Left panels correspond to central $b = 2$ fm while center and right panels refer to $b = 8$ fm. A polytrop energy loss with $(a = 1/3, z = 1, c = 8/3)$ is assumed.

$T(\vec{x}, \tau_0)(\tau_0/\tau)^{1/3}$ until a freeze-out isotherm is reached specified by $T[\vec{x}(\tau_f), \tau_f; b] = T_f = 100$ MeV. As in Refs. [32, 33], we assume that the energy loss depends monotonically on the co-moving local entropy density. We consider an initial QGP-formation time of $\tau_0 = 1$ fm/c.

The dimensionless effective jet-medium coupling κ is interpreted as proportional to α_s^3 in the case of radiative energy-loss tomography while it is interpreted to be proportional to $\kappa \propto \sqrt{\lambda_{tH}} \propto (\alpha_s N_c)^{1/2}$ in terms of the t'Hooft coupling in gravity dual string holography.

We note that the considered monotonic power-law dependence of dE/dx on the temperature (or entropy) field in Eq. (1) is a dynamical assumption consistent with pQCD tomography as well as AdS/CFT holography models in the literature. However, there also exist non-monotonic models, e.g. see Liao and Shuryak [39] involving e.g. magnetic monopole enhanced dE/dx near the critical QCD transition point of $T_c \approx 170$ MeV. The scope of the present paper is limited to monotonic models as in Eq. (1) to avoid extra model assumptions and parameters.

We note that the $(a = 1/3, z = 1, c = 8/3)$ polytrop model describes approximately both the pQCD and the AdS/CFT falling string cases [40, 41]. An $(E/T)^{1/3}$-energy dependence is numerically similar to the logarithmic $\log(E/T)$ dependence predicted by fixed coupling pQCD-energy loss in the range $10 < E/T < 600$ relevant at LHC energies. This power law is also predicted to be the lower bound of the power a in the falling-string scenario in an AdS/CFT conformal holography.

Variants of the polytrop model with path dependencies varying from $z = 1$ to $z = 2$ have been considered in Refs. [34, 35, 40–44]. Recent work [45] on the falling string energy-loss in conformal AdS geometry has identified important corrections to the original works [40, 41] that may reduce the effective $z = 2$ path-length power-law dependence assumed in [34] to $z \approx 1$ similar to the predicted radiative energy loss in pQCD. While such a falling string scenario essentially leads to the same polytrop exponents as radiative pQCD-energy loss, the jet-medium coupling strength differs significantly in the two cases.

As we also show below, Eq. (1) reduces to the survival probability model referred to as "AdS/CFT"-like in Refs. [34–36] in the limit $(a = 1, z = 2, c = 3)$. For $(a = 1, z = 0, c = 3)$, on the other hand, the polytrop model reduces to the heavy-quark string-drag energy-loss of conformal AdS holography [40, 41]. As we emphasize below, polytrops with $a = 1$ lead in fact to a generalized class of "geometric optics" or "survival probability" models of nuclear jet modifications. We will demonstrate that the recent LHC data on $R_{AA}(p_T)$ data rules out this class of dynamical models.

In this work, we further generalize Ref. [32] by using the full pQCD jet-production p_T-spectra for the initial quark and gluon jets avoiding the local spectral index approximation. In addition, we convolute the quenched jet spectra with KKP pion fragmentation functions [46] that have been tested well against RHIC $pp \to \pi^0$ spectra in Ref. [47].

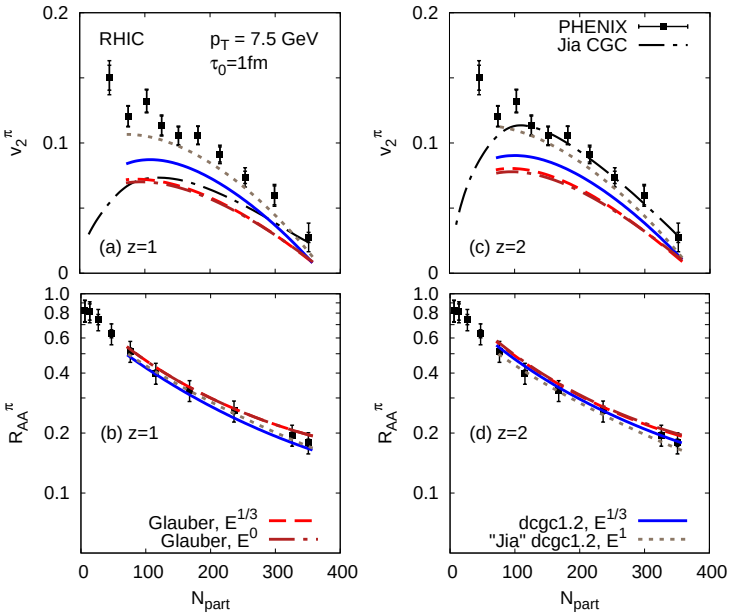

FIG. 2: (Color online) The $R_{AA}^{\pi}(N_{part})$ and the $v_2^{\pi}(N_{part})$ at RHIC energies after fragmentation for an energy loss with $z = 1$ (left panel) as well as an energy loss with $z = 2$ (right panel). Glauber initial conditions are displayed by the red dashed lines and dcgc1.2 initial conditions by the blue solid lines. Those results are obtained for $a = 1/3$. The grey dotted line represents an energy-loss for dcgc1.2 initial conditions considering just binary collisions ("Jia" dcgc1.2) as well as $a = 1$, similar to the one in Refs. [34, 35]. The dark red dashed-dotted line displays an energy loss with Glauber initial conditions and $a = 0$. All calculations assume an initialization time of $\tau_0 = 1$ fm. The black dashed-dotted line is the result for CGC initial conditions from Ref. [35].

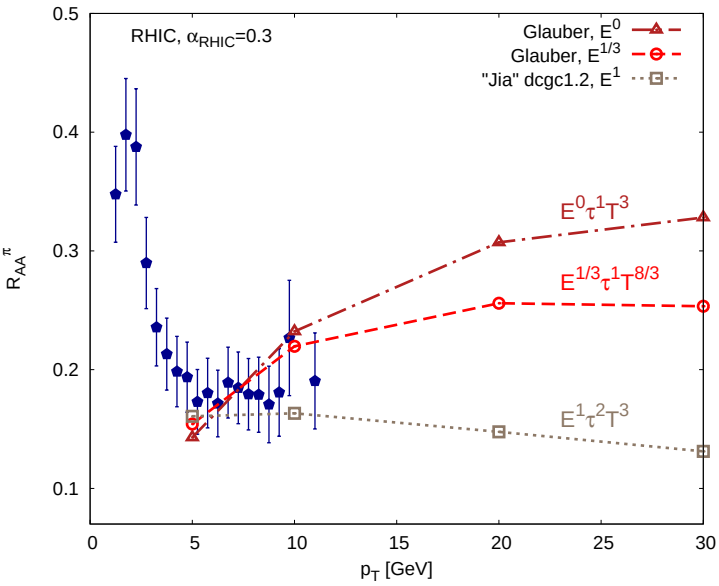

FIG. 3: (Color online) The R_{AA}^{π} at $0-5\%$ centrality as a function of p_T at RHIC energies. The grey dotted line shows an energy loss for dcgc1.2 initial conditions considering just binary collisions ("Jia" dcgc1.2) and $(a = 1, z = 2, c = 3)$, while the red dashed and dark red dashed-dotted lines dispay Glauber initial conditions for $(a = 1/3, z = 1, c = 8/3)$ and $(a = 0, z = 1, c = 3)$, respectively. The initialization time is chosen to be $\tau_0 = 1$ fm. The data are taken from Ref. [51].

The magnitude of the cube of the initial temperature profile is assumed to scale with the observed rapidity density $T_0^3(\vec{x}, b) \propto \rho(\vec{x}, b) dN_{ch}(\sqrt{s}, b)/d\eta$. The initial transverse coordinate distribution, $\rho(\vec{x}, b)$, of the QGP is modelled according to a Glauber and a higher eccentricity CGC-like elliptically deformed geometry [see Eqs.(13) to (16) below].

II. A POLYTROP MODEL OF JET-QUENCHING

At the partonic level, the nuclear modification factor R_{AA} is the ratio of the jet spectrum for jets penetrating a QGP produced in A+A collisions to the initial jet spectrum predicted by pQCD without final state interactions:

$$R_{AA}^{q,g}(P_f, \vec{x}_0, \phi) = \frac{dN_{QGP}^{jet}(P_f)}{dyd\phi dP_f^2} \Big/ \frac{dN_{vac}^{jet}(P_f)}{dyd\phi dP_0^2} = \frac{dP_0^2}{dP_f^2} \frac{dN_{vac}^{jet}[P_0(P_f)]}{dyd\phi dP_0^2} \Big/ \frac{dN_{vac}^{jet}(P_f)}{dyd\phi dP_0^2} . \quad (2)$$

Denoting the invariant jet distribution by $g_0(P)$,

$$g_0(P) = \frac{dN_{vac}^{jet}(P)}{dyd\phi dP^2} , \quad (3)$$

the nuclear modification factor for a quark (q) or gluon (g) jet with a final momentum P_f, produced at a transverse coordinate $\vec{x}_0$ and propagating in direction ϕ is, from Eq. (1),

$$R_{AA}^{q,g}(P_f, \vec{x}_0, \phi) = \frac{g_0[P_0(P_f)]}{g_0(P_f)} \frac{dP_0^2}{dP_f^2} . \quad (4)$$

The polytrop model introduced in Eq. (1) is convenient because the initial jet-parton momentum, $P_0(P_f)$ depends on the final quenched parton momentum P_f analytically as [15, 32]

$$P_0(P_f) = \left[P_f^{1-a} + K \int_{\tau_0}^{\tau_f} \tau^z T^c[\vec{x}_\perp(\tau), \tau] d\tau \right]^{\frac{1}{1-a}} , \quad (5)$$

where $K = (1-a)\kappa C_2$ for gluon(quark) jets. Non-monotonic density-dependent scenarios as in Ref. [39] can be simulated by introducing an additional local temperature-dependent function $f(T)$ inside the path integral. However, as noted in the introduction, we limit our applications to monotonic temperature dependencies of the energy loss per unit length given by T^c.

Note that if κ is dimensionless and no additional dimensionful scales influence the energy loss, the temperature exponent depends on a, c. Any deviations from the dimensional constraint

$$c = 2 - a + z \tag{6}$$

found by fitting jet systematics can be used to help identify the existence of other relevant dimensionful scales. Non-conformal physics that may modify energy loss near the cross-over temperature T_c or running coupling effects depending on $\Lambda_{QCD} \sim T_c$ could lead to violations of Eq.(6). In case of heavy-quark drag holography, $(a = 1, z = 0, c = 2)$, the sum rule is violated because of occurrence of an extra $1/M_Q$ factor of dimension -1 [40, 41].

The limit with $a = 1$ is of special interest and used frequently in the literature because it leads to a pure exponential dependence of $P_0(P_f)$:

$$P_0(P_f) = P_f \; e^{\chi_{z,c}} \tag{7}$$

with a *jet-energy independent* effective opacity

$$\chi_{z,c}(\phi) = \kappa C_2 \int_{\tau_0}^{\tau_f} d\tau \tau^z T^c(\tau, \phi)\,. \tag{8}$$

This corresponds to a generalized "geometric optics" limit with $c = 1 + z$ if no other relevant scales are involved.

In this particular case, the nuclear modification factor at the parton level then reduces to

$$R_{AA} = g_0(P_f \; e^{\chi}) \; e^{2\chi}/g_0(P_f)\,. \tag{9}$$

Approximating the initial jet spectrum by a simple power law, $g_0 \propto p^{-n}$, where n is the jet spectral index, the nuclear modification factor reduces to the simplest possible *energy independent* "jet survival probability" in azimuthal direction ϕ given by

$$R_{AA}(\phi) = e^{(2-n)\chi_{z,c}(\phi)} = e^{-\chi_{eff}(\phi)} \equiv P_0(\phi)\,. \tag{10}$$

Since at both RHIC and LHC the spectral indices of quarks and gluons differ and vary significantly with the jet energy, we must use Eq. (9) rather than the naive constraint of Eq. (10) to explore the consequences of $a = 1$ energy loss models.

For the general (a, z, c) case, we use Eqs. (4) and (5) to compute the parton level nuclear modification factor. The final pion nuclear modification reads

$$R^{\pi}_{AA}(p_\pi, \phi) \;=\; = \frac{\sum\limits_{\alpha=q,g} \int\limits_{z_{min}}^{1} \frac{dz}{z}\, d\sigma_\alpha\left(\frac{p_\pi}{z}\right) R^{\alpha}_{AA}\left(\frac{p_\pi}{z}, \phi\right) D_{\alpha\to\pi}\left(z, \frac{p_\pi}{z}\right)}{\sum\limits_{\alpha=q,g} \int\limits_{z_{min}}^{1} \frac{dz}{z}\, d\sigma_\alpha\left(\frac{p_\pi}{z}\right) D_{\alpha\to\pi}\left(z, \frac{p_\pi}{z}\right)}\;, \tag{11}$$

with $z_{min} = \frac{2p_\pi}{\sqrt{s}}$. The parton level R^{α}_{AA} is averaged over the initial jet production geometry in a given centrality class. We use the KKP pion fragmentation functions [46] that have been successfully tested on the $pp \to \pi^0$ spectra at RHIC and LHC.

Figure 1 shows the partonic level R_{AA} and v_2 as a function of p_T for gluons (red dashed-dotted lines) and quarks (blue dashed lines) prior to fragmentation, as well as for pions (black solid lines) after fragmentation for a $(a = 1/3, z = 1, c = 8/3)$ polytrop energy loss and Glauber initial conditions. The upper panel displays RHIC and the lower panel LHC energies where the coupling κ was reduced to fit the central 0-5% $R^{\rm LHC}_{AA}$ reference point at $p_T = 10$ GeV. The purpose of this figure is simply to demonstrate the remarkable similarity of quenched pion and quenched quark jets at both RHIC and LHC in spite of the much higher number of initial gluon jets especially at LHC.

As can be seen from Fig. 1, the pion nuclear modification factor is completely dominated by quark quenching and fragmentation at both RHIC and LHC energies due to the fact that the gluon-energy loss is enhanced by a factor of 9/4. The dominance of the quenched quark fragmentation reduces the sensitivity to the fragmentation function uncertainties because quark fragmentation functions are the best constrained experimentally.

From the calculated $R^{\pi}_{AA}(p_\pi, \phi) = R^{\pi}_{AA}(p_\pi, N_{part}, \phi)$ one obtains the centrality dependent $R^{\pi}_{AA}(N_{part})$ for a given p_π by averaging over the azimuthal angles ϕ [32]. Then, the $v_2(N_{part})$ is computed via

$$v_2^{\pi}(N_{part}) \;=\; \frac{\int d\phi \cos\{2\phi\}\; R^{\pi}_{AA}(N_{part}, \phi)}{\int d\phi\, R^{\pi}_{AA}(N_{part}, \phi)}\,. \tag{12}$$

We fix the value of jet-medium coupling κ at RHIC energies in each case by fitting to the same one reference point with $R_{AA}(p_T = 7.5 \text{ GeV}) \approx 0.2$ in central 0-5% collisions.

Glauber participant and binary collision initial condition geometries are computed using the Monte Carlo model introduced in Ref. [32]. To simulate CGC-like higher eccentricity initial conditions, we simply deform the Glauber initial geometry via the rescaling:

$$x \to s_x x, \quad y \to s_y y\,, \tag{13}$$

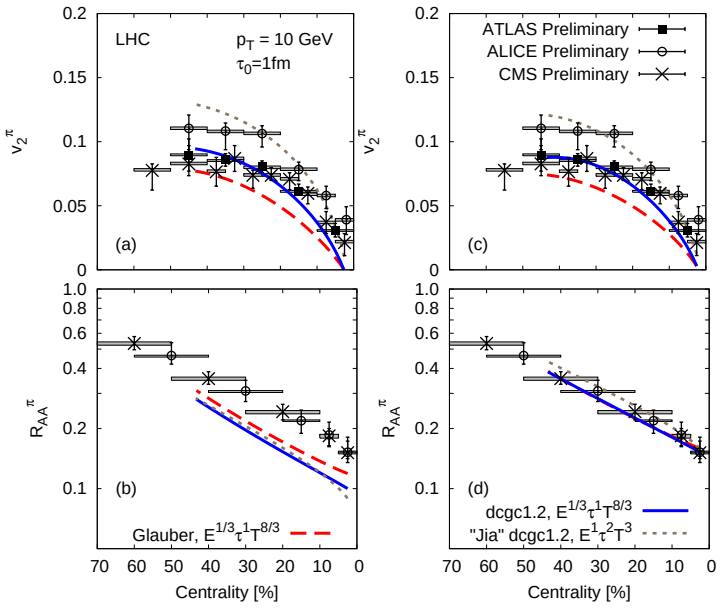

FIG. 4: (Color online) The R_{AA}^{π}(Centr.) and the v_2^{π}(Centr.) at LHC energies after fragmentation, considering either the same coupling as for RHIC energies (left panel), or a reduced coupling (right panel). Here we compare Glauber initial conditions (red dashed lines) and dcgc1.2 initial conditions (blue solid lines) for an $(a = 1/3, z = 1, c = 8/3)$ energy-loss with a scenario for dcgc1.2 initial conditions considering just binary collisions ("Jia" dcgc1.2) and $(a = 1, z = 2, c = 3)$ (grey dotted lines). Data are taken from Refs. [10, 53–56].

where the scaling factors are determined by fitting tabulated Glauber and MC-KLN second moments as a function of b:

$$s_x = \sqrt{\frac{\langle x^2\rangle_{\rm CGC}}{\langle x^2\rangle_{\rm Gl}}}, \quad s_y = \sqrt{\frac{\langle y^2\rangle_{\rm CGC}}{\langle y^2\rangle_{\rm Gl}}}\,. \tag{14}$$

Here, $\langle\circ\rangle$ denotes the geometric average at a given b. Assuming that the ratios of eccentricities ($\epsilon = e_2$) and the root-mean-square ($r^2 =< x^2+y^2 >$) for Glauber and CGC initial conditions can be expressed via $\epsilon_{\rm CGC} = f\cdot\epsilon_{\rm Gl}$ and $\mathrm{r}^2_{\rm CGC} = g\cdot \mathrm{r}^2_{\rm Gl}$, we found that deformations with $f = 1.2\pm0.1$ and $g = 0.95\pm0.05$ reproduce the numerical MC-KLN tables of Jia very well [50].

In the following, we will refer to the deformed CGC geometry corresponding to $(f = 1.2, g = 0.95)$ as "dcgc1.2". Please note that the Glauber geometry applied corresponds to 86% participant plus 14% binary fraction. Given (f, g), the deformed CGC geometry has mean in-plane and out-of-(reaction)-plane moments of

$$\begin{aligned}\langle x^2\rangle_{\rm CGC} &= g\,\mathrm{r}^2_{\rm Gl}(1 - f\,\epsilon_{\rm Gl})/2\\ \langle y^2\rangle_{\rm CGC} &= g\,\mathrm{r}^2_{\rm Gl}(1 + f\,\epsilon_{\rm Gl})/2\,.\end{aligned} \tag{15}$$

The energy-density field transforms under this elliptic deformation as

$$\tilde\epsilon(x,y) = \epsilon\left(\frac{x}{s_x},\frac{y}{s_y}\right)\left(\frac{1}{s_x s_y}\right)^{4/3}. \tag{16}$$

We checked that the temperature profiles and eccentricities of this azimuthally deformed Glauber model coincide with the ones of the fKLN model of Drescher et. al. [30, 31].

In addition, we will also consider a QGP geometry that corresponds to deformed Glauber initial conditions that are based on pure binary collisions which leads to a larger eccentricity. We will refer to that enhanced eccentricity geometry as "Jia" dcgc1.2 as this geometry, together with $a = 1$, reproduces the PHENIX v_2-data reviewed below.

Since we showed in Ref. [32] that event-by-event geometrical fluctuations lead to very similar R_{AA} and v_2 as event-averaged geometries, we consider only the event-averaged geometries in this paper.

III. RESULTS AND DISCUSSION

Figure 2 shows the centrality dependence of $R^{\pi}_{AA}(N_{part})$ (lower panels) and $v^{\pi}_2(N_{part})$ (upper panels) for pions with $p_T = 7.5$ GeV at RHIC energies considering a polytrop energy-loss scenario with $z = 1$ (left panel) and $z = 2$ (right panel) for three $(a, z, c = 2 - a + z)$ models. Red dashed lines correspond to Glauber initial conditions for a pQCD-like scenario with $(a = 1/3, z = 1, c = 8/3)$ as shown in the left panel, while a hybrid quadratic path-length dependence with $(a = 1/3, z = 2, c = 11/3)$ is displayed in the right panels. Note that there is virtually no dependence on the z exponent and for both scenarios, the results for the elliptic flow fall below the PHENIX data. The same polytrops for the deformed $(f = 1.2, g = 0.95)$ dcgc1.2 CGC-like geometry are shown in solid blue. The enhanced eccentricity increases the predicted $v_2(p_T = 7.5\,\mathrm{GeV}, N_{part})$ but the solid blue curves remain well below the v_2-data. Therefore, neither geometries nor linear $(z = 1)$ or quadratic $(z = 2)$ path dependences account for the PHENIX data considering our default pQCD-like $E^{1/3}$ polytrop case.

The long dashed-dotted black curves represents to the results of the "survival probability" model used in Refs. [34, 35]. That model fits remarkably well both the centrality dependence of R_{AA} and v_2 simultaneously at the reference of $p_T = 7.5$ GeV. This model, corresponds to the doubly special limit [Eq. (10)] of the more general "geometrical optics" $(a = 1, z = 2, c = 3)$ case given by Eq. (9). However, since the spectral index is not constant as a function of p_T at RHIC, this double limit is not consistent.

Therefore, we also show the dotted grey lines in Fig. 2 using the full spectral shape with Eq. (11) and corresponding to $dE/dx \propto E^1$. Applying the high eccentricity "Jia" dcgc1.2 geometry of Refs. [34, 35], we find that Eq. (11) results in $v_2(p_T = 7.5\,\mathrm{GeV}, N_{part})$ close to Jia's curve and the data.

The results for $a = 1/3$ are comparable to those shown in Ref. [32] where, however, the full convolution over the parton spectra and pion fragmentation functions was not

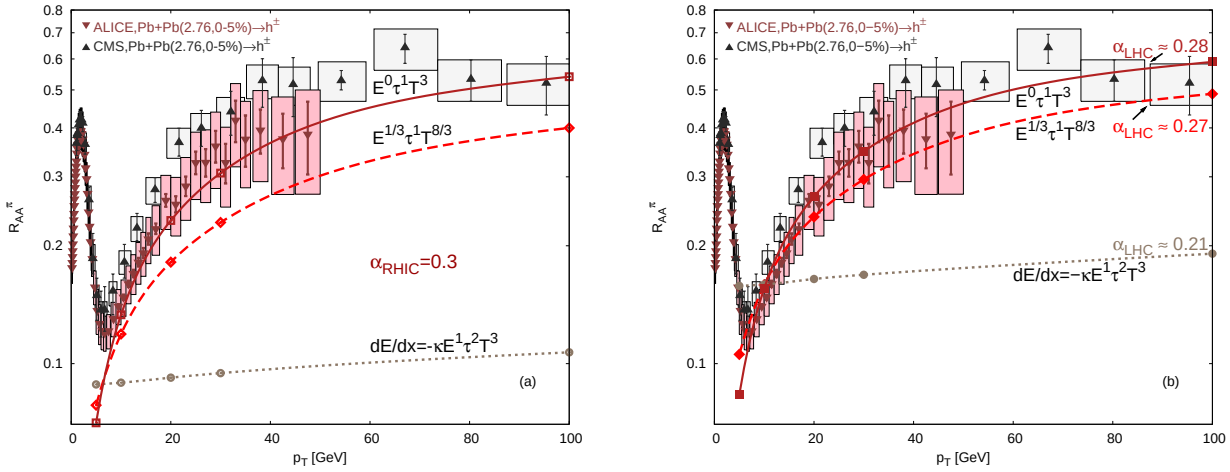

FIG. 5: (Color online) The nuclear modification factor of pions at $0-5\%$ centrality as a function of p_T, shown for LHC energies, assuming either the same coupling as at RHIC energies (left panel) or a reduced coupling (right panel). The plot contrasts an energy-loss scenario for dcgc1.2 initial conditions considering just binary collisions ("Jia" dcgc1.2, grey dotted lines) for $(a = 1, z = 2, c = 3)$ with energy-loss scenarios for Glauber initial conditions and $(a = 1/3, z = 1, c = 8/3$; red dashed lines) or $(a = 0, z = 1, c = 3$; dark red solid lines), respectively. The data are taken from Refs. [10, 53, 56].

performed.

We note that the fKLN model used in Ref. [32] appeared to reproduce the data for $z = 2$, but we discovered that the numerics of the fKLN code used was not stable to small variations of parameter settings. This is the reason we abandoned the fKLN calculations in this work and chose instead to compare Glauber to deformed Glauber dcgc1.2 geometries. Our conclusion with new deformed geometry is that $a = 1/3$ polytrops underestimate v_2 at RHIC independent of path-length dependence.

If the simple geometric optics model with $(a = 1)$ is the correct explanation of v_2-data, then the $R_{AA}(p_T)$ should be approximately independent of p_T as can be seen from Eq. (11). In Fig. 3 this prediction is compared to RHIC data. We note that the curve for $(a = 1, z = 2, c = 3)$ deceases slightly due to using the full spectral shape as well as the convolution over the pion fragmentation functions. Current RHIC data are indeed consistent with an approximately p_T independence in the $5 < p_T < 10$ GeV window, but the large systematic errors beyond 10 GeV prevent a stringent test of this flatness. As seen from the figure, even $a = 0, 1/3$ energy exponents are consistent within the error bars. Future higher statistics measurements at RHIC in the range $5 < p_T < 30$ GeV are obviously needed to differentiate between the energy-loss models.

Having constrained the coupling of different polytrop models at RHIC, we turn to the predictions of these models for LHC conditions in Figs. 4 and 5. Here, the LHC data are taken from Refs. [10, 53–55]. In Eq. (11) we use the parton spectra predicted by pQCD as well as the doubling of the density between RHIC and LHC. We scale the temperature field used in Eq. (5) by a factor $(2.2)^{1/3}$ relative to RHIC.

Fig. 4(b) is one of the main results showing that all three RHIC constrained polytrop models shown in Fig. 3 overpredict the LHC nuclear modification factor for most central collisions at the LHC-reference point of $p_T = 10$ GeV. Thus, we find in Fig. 4(b) that our extrapolation from RHIC to LHC conditions assuming the same jet-medium coupling as the density increases by a factor of ~ 2.2 from RHIC to LHC underpredicts the observed $R_{PbPb}(p_T = 10\,\mathrm{GeV}, 0-5\%)$ at all centralities and that this discrepancy is robust to substantial variations of the (a, z, c) exponents of the energy-loss model assumed. This results extends the robustness of the evidence for a reduced jet-medium coupling at LHC found in Refs. [15–17] to a much broader class of models.

The main result found in Fig. 2 was that the measured $R^{\pi}_{AA}(N_{\mathrm{part}})$ and $v^{\pi}_2(N_{\mathrm{part}})$ at RHIC at $p_T = 7.5$ GeV appears to be best described with a polytrop model for $(a = 1, z = 2, c = 3)$. The predicted p_T-flatness of the nuclear modification factor shown in Fig. 3 is also consistent with the measured data. However, we by comparing with LHC data in Fig. 5 we learn that the $dE/dx \propto E^1$ dynamics is completely falsified by the rising $R_{AA}(p_T)$ at RHIC energies which is independent of the magnitude of the jet-medium coupling.

Fig. 5b, in which the jet-medium couplings of the three different polytrops are reduced to fit the 10 GeV reference point at most central collisions, clearly shows that, within the current experimental uncertainties, the rapid rise of the $R_{AA}(p_T)$ at the LHC rules out any energy-loss model with an exponent $a > 1/3$. In fact, the data appear to slightly favor the $a = 0$ case.

As a further consistency test we compare the centrality dependence of the $R^{Pb+Pb}_{AA}(5 < p_T < 30\,\mathrm{GeV})$ for the polytrop model with $(a = 1/3, z = 1, c = 8/3)$ in Fig. 6 [53] to ALICE data. The observed agreement between data and model calculations is in fact to robust to

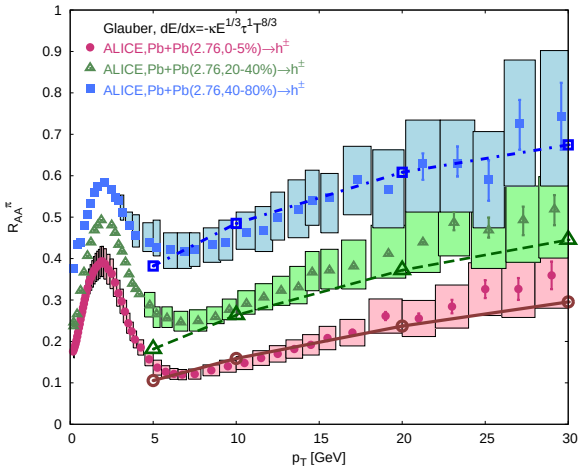

FIG. 6: (Color online) The nuclear modification factor of pions as a function of p_T for $0-5\%$ (solid magenta line), $20-40\%$ (dashed green line), and $40-80\%$ centralities (dashed-dotted blue line) at LHC energies, compared to an energy-loss scenario of $(a=1/3, z=1, c=8/3)$. Results are computed assuming Glauber geometry but R_{AA} curves with dcgc1.2 (not shown) were found to be essentially the same. The centrality classes are computed with the same reduced coupling determined from the most central $p_T = 10$ GeV reference point. The data are taken from Ref.[53].

changes between Glauber and deformed dcgc1.2 geometries for initial conditions.

Since our results support the conclusion that the QGP created at LHC appears more transparent than expected based on fixed-coupling extrapolations from RHIC [15, 17], it is important to try to quantify the magnitude of the reduction needed to obtain the agreement shown in Fig. 4(d). The ratio of the coupling needed to reproduce the LHC reference point to the one that fits the RHIC data provides a useful measure of the degree of weakening of the effective jet-medium coupling as the QGP density doubles from RHIC to LHC.

In pQCD radiative energy loss, $\kappa \propto \alpha^3$ and the strong coupling thus scales from RHIC to LHC as

$$\alpha_{\rm LHC} \;=\; (\kappa_{\rm LHC}/\kappa_{\rm RHIC})^{1/3}\;\alpha_{\rm RHIC}\,, \qquad (17)$$

where $\alpha_{\rm RHIC} \sim 0.3$. Inserting the values used in Fig. 4, which are summarized in Table I for the $z=1$ energy loss shown as well as a $z=2$ energy loss not shown here in detail, we find that $\alpha_{\rm LHC} \sim 0.24-0.27$ for an energy-loss scenario of $a=1/3$, indicating a plausible moderate reduction of the pQCD coupling due to slow running (creeping) above the deconfinement temperature (see also Ref. [15–17]), while for the "Jia" optical limit $\alpha_{\rm LHC} \sim 0.21$ and for $(a=0, z=1, c=3)$ $\alpha_{\rm LHC} \sim 0.28$. Remarkably, by comparing the values for $a=1/3$ in Table I with Table II, we find that the ratio of LHC to RHIC effective couplings is insensitive to the assumed τ_0 in the range 0-1 fm/c.

On the other hand, in the falling-string scenario [40, 41, 43–45], the effective jet-medium coupling $\kappa \propto \sqrt{\lambda}$ is related to the square root of the t'Hooft coupling $\lambda = g^2_{YM} N_c$. Gravity-dual descriptions require that $\lambda \gg 1$. For heavy-quark quenching, it was found in Ref. [25] that large $\lambda_{\rm RHIC} \sim 20$ provides a reasonably good fit to the RHIC data as well as to the bulk v_2 elliptic flow.

In the falling string scenario, $\lambda_{\rm LHC}$ and $\lambda_{\rm RHIC}$ are then related via

$$\lambda_{\rm LHC} \;=\; (\kappa_{\rm LHC}/\kappa_{\rm RHIC})^2\;\lambda_{\rm RHIC}\,. \qquad (18)$$

From the holographic point of view, Tables I and II imply that $\lambda_{\rm LHC}$ must be reduced by a rather large factor of $\sim 2-4$ relative to RHIC for the $a=1/3$ scenario and an even larger factor of ~ 10 for the optical "Jia" limit. This result implies a rather strong breaking of conformal symmetry over a narrow temperature interval. It is not yet clear if current non-conformal holographic models are consistent with such a strong variation (see, for example, Refs. [44, 52]).

Figs. 2 and 4 already showed that there is a remarkably insensitivity of the elliptic flow to the initial conditions and the strength of the coupling constant [compare e.g. Fig. 4(a) with Fig. 4(b)]. Fig. 7 demonstrates elliptic flow measurements at LHC, which recently are in remarkable agreement between ATLAS, ALICE, and CMS [53–55] will not allow for a disentangling of Glauber vs.

Effective Coupling κ assuming $\tau_0 = 1.0$ fm/c					
$\sqrt{s}$	Glauber a=1/3 z=1	dcgc1.2 a=1/3 z=1	Glauber a=1/3 z=2	Glauber a=0 z=1	"Jia" a=1 z=2
0.20	0.93	1.09	0.55	3.30	0.057
2.76	0.66	0.66	0.33	2.72	0.017
LHC/RHIC	0.71	0.61	0.60	0.82	0.33

TABLE I: The effective coupling κ at RHIC and LHC energies for Glauber and dcgc1.2 initial conditions and $\tau_0 = 1.0$ fm/c. The last row displays the ratio $\kappa_{LHC}/\kappa_{RHIC}$.

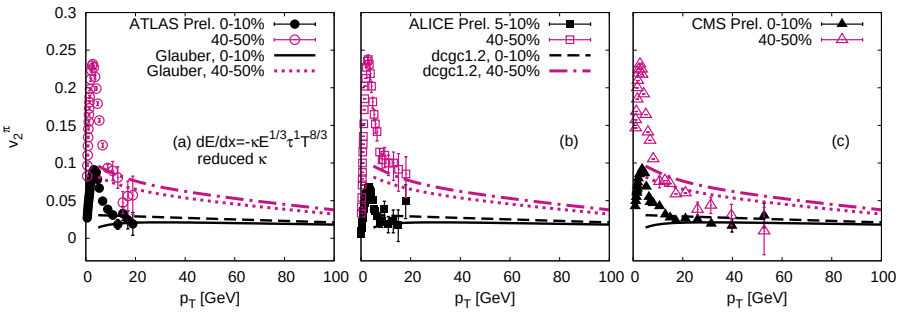

FIG. 7: (Color online) v_2^π as a function of p_T, shown for different centralities at LHC energies for an energy loss with ($a = 1/3, z = 1, c = 8/3$), compared to ATLAS (left panel), ALICE (middle panel), and CMS data (right panel) for central (full symbols) and peripheral collisions (open symbols). Glauber initial conditions are displayed by the solid black and dotted magenta lines while the dcgc1.2 initial conditions are represented by the dashed black and dashed-dotted magenta lines. Here, the initialization time is chosen to be $\tau_0 = 1$ fm and a reduced coupling constant is assumed as compared to RHIC energies. The data are taken from Refs. [54, 55, 57].

Effective Coupling κ assuming $\tau_0 = 0.01$ fm/c			
$\sqrt{s}$	Glauber z=1	dcgc1.2 z=1	Glauber z=2
0.20	0.60	0.58	0.44
2.76	0.45	0.43	0.26
LHC/RHIC	0.75	0.74	0.59

TABLE II: Same as table I but for fits assuming $\tau_0 = 0.01$ fm/c.

dcgc1.2 initial conditions. Preliminary data from CMS up to $p_T \sim 50$ GeV [57] (right panel of Fig. 7) show that the the elliptic flow for central collisions indeed stays flat for high momenta while v_2^π for more peripheral collisions decreases slowly approaching the value for central collisions.

IV. SUMMARY

Using a generic, polytrop power-law model of energy, path-length, and monotonic density dependence characterized by the three exponents (a, z, c) that can interpolate between a wide class of weakly and strongly-coupled jet-medium interactions, we investigated those interactions as well as the jet-medium coupling at both RHIC and LHC energies for Glauber and CGC-like, deformed Glauber (dcgc1.2) initial conditions.

We found that at RHIC energies the measured data for the nuclear modification factor and the elliptic flow as a function of centrality are best described by the scenario with ($a = 1, z = 2, c = 3$) that also describes the flatness of the $R_{AA}^{\rm RHIC}(p_T)$.

However, this energy-loss model is completely falsified at LHC energies because it does not describe the rising of the $R_{AA}^{\rm LHC}(p_T)$. In fact, the rapid rise of the nuclear modification factor rules out any energy-loss model with an energy exponent $a > 1/3$ and slightly favors the $a = 0$ case.

Moreover, we find that an extrapolation from RHIC to LHC energies leads to an underprediction of the nuclear modification factor [15–17], independently of the (a, z, c) exponents assumed, emphasizing the robust evidence for a reduced jet-medium coupling at the LHC. We showed that in terms of pQCD a moderate reduction of the effective jet-medium coupling with $\alpha_{LHC} \sim 0.24 - 0.28$ relative to RHIC ($\alpha_{RHIC} = 0.3$) allows to describe both the nuclear modification factor and the elliptic flow as a function of centrality and as a function of p_T. Thus, the LHC data are compatible with $0 \leq a \leq 1/3$ pQCD-like energy-loss models where the jet-medium coupling is reduced by approximately 10% between RHIC and LHC.

In terms of strongly-coupled holographic models, however, our LHC fit requires a much larger reduction of the effective t'Hooft coupling from $\lambda_{\rm RHIC} \sim 20$ by a factor of $2-4$ to $\lambda_{\rm LHC} \sim 5-10$. This suggests that stronger non-conformal effects must be considered for a holographic phenomenology of the LHC.

We found that both Glauber and CGC-like, deformed Glauber (dcgc1.2) initial conditions describe the centrality dependence of the nuclear modification factor $R_{AA}^\pi(p_T)$ and the elliptic flow v_2^π well for RHIC and LHC energies which does not allow us to disentangle the initial conditions using those two observables.

As demonstrated in Fig. 1, the nuclear modification factor as well as the elliptic flow at both RHIC and LHC energies for $p_T > 5$ GeV are dominated by quark jet-quenching and fragmentation because gluon jets are strongly quenched and fragmentation leads to pions with a smaller fractional momentum. This underlines the conclusion of Ref. [17] that single-hadron jet-flavor tomography observables are mainly sensitive to quark rather than gluon jet-medium interactions. The reduced jet-medium coupling quantified in this work therefore primarily refers to the apparent weakening of quark-jet interactions in a QGP when the density approximately doubles from RHIC to LHC. It remains a challenge to identify jet ob-

servables more sensitive to gluon jet-quenching to test color Casimir scaling currently assumed in both weakly-coupled pQCD tomography and strongly-coupled string holography. Di-hadron and jet-shape observables could help to probe gluon versus quark jet-medium interactions in the future.

Acknowledgements

M.G. and B.B. acknowledge support from DOE under Grant No. DE-FG02-93ER40764. B.B. is supported by the Alexander von Humboldt foundation via the Feodor Lynen program. The authors thank G. Torrieri, J. Jia, A. Buzzatti, A. Ficnar, W. Horowitz, J. Liao, M. Mia, J. Noronha, J. Harris, G. Roland, B. Cole, and W. Zajc for extensive and fruitful discussions.

[1] K. Aamodt [ALICE Collaboration], Phys. Lett. B **696**, 30 (2011).
[2] J. Otwinowski [ALICE Collaboration], J. Phys. G G **38**, 124112 (2011).
[3] H. Appelshauser and f. t. A. Collaboration, J. Phys. G G **38**, 124014 (2011).
[4] G. C. B. f. t. A. collaboration, J. Phys. G G **38**, 124117 (2011).
[5] J. Schukraft and f. t. A. Collaboration, J. Phys. G G **38**, 124003 (2011).
[6] A. Dainese and f. t. A. Collaboration, J. Phys. G G **38**, 124032 (2011).
[7] [ATLAS Collaboration], Phys. Lett. B **710**, 363 (2012).
[8] P. Steinberg and A. Collaboration, J. Phys. G G **38**, 124004 (2011).
[9] J. J. f. t. A. Collaboration, J. Phys. G G **38**, 124012 (2011).
[10] CMS Collaboration, Physics Analysis Summary (PAS), http://cdsweb.cern.ch/record/1347788?ln=en.
[11] A. S. Y. f. t. C. collaboration, arXiv:1107.1862 [nucl-ex].
[12] S. Chatrchyan *et al.* [CMS Collaboration], JHEP **1108**, 141 (2011).
[13] S. Chatrchyan *et al.* [CMS Collaboration], JHEP **1107**, 076 (2011).
[14] S. Chatrchyan *et al.* [CMS Collaboration], Phys. Rev. C **84**, 024906 (2011).
[15] W. A. Horowitz and M. Gyulassy, Nucl.Phys. A872 (2011) 265.
[16] B. G. Zakharov, JETP Lett. **93**, 683 (2011).
[17] A. Buzzatti and M. Gyulassy, Phys. Rev. Lett. **108**, 022301 (2012).
[18] I. Vitev, J. Phys. G G **38**, 124087 (2011).
[19] M. Gyulassy and L. McLerran, Nucl. Phys. A **750**, 30 (2005); E. V. Shuryak, Nucl. Phys. A **750**, 64 (2005).
[20] I. Arsene *et al.* [BRAHMS Collaboration], Nucl. Phys. A **757**, 1 (2005).
[21] B. B. Back *et al.*, Nucl. Phys. A **757**, 28 (2005).
[22] J. Adams *et al.* [STAR Collaboration], Nucl. Phys. A **757**, 102 (2005).
[23] K. Adcox *et al.* [PHENIX Collaboration], Nucl. Phys. A **757**, 184 (2005).
[24] J. M. Maldacena, Adv. Theor. Math. Phys. **2**, 231-252 (1998).
[25] J. Noronha, M. Gyulassy and G. Torrieri, Phys. Rev. C **82**, 054903 (2010).
[26] M.Gyulassy, Physics 2, (2009) 107.
[27] M. L. Miller, K. Reygers, S. J. Sanders and P. Steinberg, Ann. Rev. Nucl. Part. Sci. **57**, 205 (2007).
[28] E. Iancu and R. Venugopalan, arXiv:hep-ph/0303204.
[29] D. Kharzeev and E. Levin, Phys. Lett. B **523**, 79 (2001).
[30] H. J. Drescher, A. Dumitru, C. Gombeaud and J. Y. Ollitrault, Phys. Rev. C **76**, 024905 (2007).
[31] H. J. Drescher, A. Dumitru, A. Hayashigaki and Y. Nara, Phys. Rev. C **74**, 044905 (2006).
[32] B. Betz, M. Gyulassy, G. Torrieri, Phys. Rev. **C84**, 024913 (2011).
[33] B. Betz, M. Gyulassy and G. Torrieri, J. Phys. G G **38**, 124153 (2011).
[34] A. Drees, H. Feng and J. Jia, Phys. Rev. C **71**, 034909 (2005); J. Jia and R. Wei, Phys. Rev. C **82**, 024902 (2010).
[35] A. Adare *et al.* [PHENIX Collaboration], Phys. Rev. Lett. **105**, 142301 (2010).
[36] J. Jia, W. A. Horowitz and J. Liao, Phys. Rev. C **84**, 034904 (2011).
[37] R. J. Fries and R. Rodriguez, Nucl. Phys. A **855**, 424 (2011).
[38] J. D. Bjorken, Phys. Rev. D **27**, 140 (1983).
[39] J. Liao, arXiv:1109.0271 [nucl-th]; J. Liao and E. Shuryak, Phys. Rev. Lett. **102**, 202302 (2009).
[40] S. S. Gubser, D. R. Gulotta, S. S. Pufu and F. D. Rocha, JHEP **0810**, 052 (2008).
[41] P. M. Chesler, K. Jensen, A. Karch and L. G. Yaffe, Phys. Rev. D **79**, 125015 (2009).
[42] P. M. Chesler, K. Jensen and A. Karch, Phys. Rev. D **79**, 025021 (2009).
[43] P. Arnold and D. Vaman, JHEP **1104**, 027 (2011).
[44] A. Ficnar, J. Noronha and M. Gyulassy, J. Phys. G G **38**, 124176 (2011); Nucl. Phys. A **855**, 372 (2011).
[45] A. Ficnar, arXiv:1201.1780 [hep-th].
[46] B. A. Kniehl, G. Kramer and B. Potter, Nucl. Phys. B **597**, 337 (2001).
[47] F. Simon [STAR Collaboration], AIP Conf. Proc. **870** (2006) 428.
[48] H. Song, S. A. Bass, U. Heinz, T. Hirano and C. Shen, Phys. Rev. Lett. **106**, 192301 (2011).
[49] B. Alver and G. Roland, Phys. Rev. C **81**, 054905 (2010).
[50] J. Jia, private communication.
[51] A. Adare *et al.* [PHENIX Collaboration], Phys. Rev. Lett. **101**, 232301 (2008).
[52] M. Mia, K. Dasgupta, C. Gale and S. Jeon, J. Phys. G G **39**, 054004 (2012); M. Mia and C. Gale, Nucl. Phys.

A **830**, 303C (2009).
[53] B. Abelev *et al.* [ALICE Collaboration], arXiv:1205.5761 [nucl-ex].
[54] R. S. f. t. A. Collaboration, J. Phys. G G **38**, 124013 (2011).
[55] J. J. f. t. A. Collaboration, J. Phys. G G **38**, 124012 (2011).
[56] S. Chatrchyan *et al.* [CMS Collaboration], arXiv:1202.2554 [nucl-ex].
[57] CMS Collaboration, CMSPublic Web, https://twiki.cern.ch/twiki/bin/view/CMSPublic/PhysicsResultsHIN11012.